

# Cosmic Rays above the Knee

Michael Unger\*

\*Karlsruher Institut für Technologie (KIT)  
Postfach 3640, D-76021 Karlsruhe, Germany  
Email: Michael.Unger@kit.edu

**Abstract**—An overview on the present observational status and phenomenological understanding of cosmic rays above  $10^{16}$  eV is given. Above these energies the cosmic ray flux is expected to be gradually dominated by an extra-galactic component. In order to investigate the nature of this transition, current experimental activities focus on the measurement of the cosmic ray flux and composition at the 'ankle' or 'dip' feature at several EeV. At the ultra high energy end of the spectrum, the flux suppression above 50 EeV is now well established by the measurements of HiRes and the Pierre Auger Observatory and we may enter the era of charged particle astronomy.

## I. INTRODUCTION

The all particle spectrum of cosmic rays is known to follow a power law,  $dN/dE \propto E^{-\gamma}$  over many orders of magnitude. However, at the highest energies, shown in Fig. 1, it exhibits three remarkable features. The *knee* [1], a steepening of the flux by  $\Delta\gamma \approx 0.5$ , at a few PeV followed by a flattening called the *ankle* [2] at several EeV and a flux suppression at ultra high energies [3].

The first two features are suspected to be an indication of the end of the galactic cosmic ray spectrum and the transition to an extra-galactic component.

At energies above several hundreds of TeV the particle fluxes are too low to allow for a direct measurement of the properties of cosmic rays. Instead, as will be explained in Sec. II, the analysis of *air showers* plays a crucial role to measure their flux and composition. These two observables are essential to study the transition from galactic to extra-galactic cosmic rays and to distinguish between the various models put forward to explain the ankle (see Sec.III and IV).

At the same hour this talk was given, the first proton beams were injected to the Large Hadron Collider [4], that will eventually be able to accelerate protons up to  $7 \cdot 10^{12}$  eV. The ultra-high energy frontier of physics is however beyond  $10^{20}$  eV, where several cosmic rays have already been detected [5]–[7]. At these extreme energies, particles are expected to suffer significant energy losses during their propagation to earth. The corresponding flux suppression was predicted over forty years ago [3] and it is only now, that experiments gathered enough statistics to study it carefully (see Sec. V).

The astrophysical sources that are able to accelerate particles to such tremendous energies are still unknown. Their unambiguous identification requires to study the arrival directions of cosmic rays, i.e. to do *particle astronomy*.

Whereas the experimental knowledge on cosmic rays made a major leap forward in the current *hybrid era* [8], new

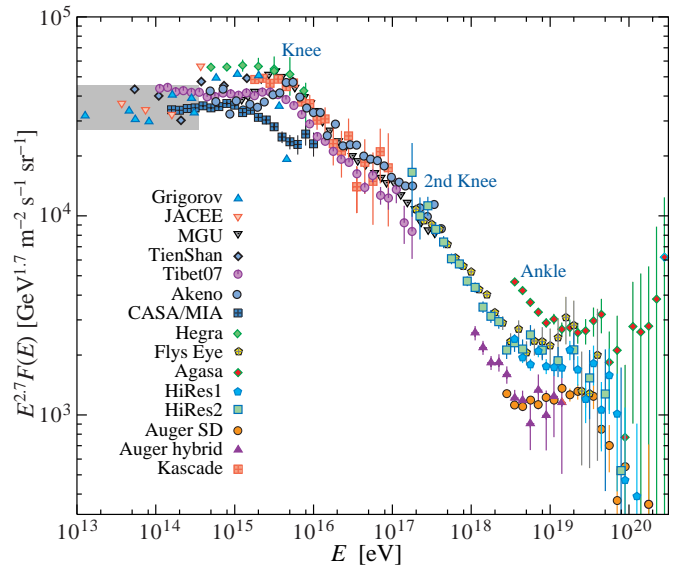


Fig. 1. All particle flux of cosmic rays ([10] and references therein)

projects aim to accumulate more data below 1 EeV and at ultra high energies. Moreover, new data on hadronic interactions at man-made particle accelerators are needed to facilitate the interpretation of air shower data [9]. These efforts will be described in Sec. VI.

## II. AIR SHOWERS

Cosmic particles entering the earth's atmosphere sooner or later collide with the nuclei of the air and initiate a particle cascade, the so-called air shower. Since the thickness of the atmosphere is more than 20 radiation and interaction lengths at vertical incident, it constitutes a suitable calorimeter to study the properties of the primary cosmic ray particles.

Air shower detectors either measure the lateral densities of particles at ground or the longitudinal development of the cascade in the atmosphere.

The qualitative relation of these experimental observables to the energy  $E_0$  and mass  $A$  of the primary particle can be easily understood within the simple Heitler-model [11]–[14] of air showers. Here one assumes that after each hadronic interaction length,  $\lambda$ ,  $\pi$ -mesons are produced with an average multiplicity of  $\langle n \rangle$ . In each interaction an energy fraction of  $f \approx 1/3$  goes to neutral pions which decay immediately into

two photons and thus feed the electromagnetic component of an air shower, that develops through pair-production and bremsstrahlung until the energy of electromagnetic secondaries falls below the critical energy  $\epsilon_{em}$  ( $\approx 81$  MeV in air). In that way, the fraction of the primary energy in the electromagnetic component at the  $n$ th interaction at depth  $n \cdot \lambda$  increases to  $1 - (1 - f)^n$  until the energy of the charged pions falls below the critical energy  $\epsilon_{ch}$  at which their decay length becomes smaller than the interaction length. If one furthermore assumes that a nucleus with mass  $A$  and energy  $E_0$  is equivalent to  $A$  nucleons of energy  $E_0/A$  (the so-called *superposition model*), the following important relations can be deduced from this simplistic model:

The average depth at which the electromagnetic cascade reaches its maximum,  $\langle X_{max} \rangle$ , grows logarithmically with the energy per nucleon:

$$\langle X_{max} \rangle = a + b \lg [(E_0/\epsilon_{em})/A], \quad (1)$$

where the constants  $a$  and  $b$  depend on the properties of hadronic interactions,  $f$ ,  $\lambda$  and  $\langle n \rangle$ . Since most of the energy of the primary particle eventually ends up in the electromagnetic cascade, the integral electron number is a good estimator for  $E_0$ . Hence, the observation of the longitudinal development of an air shower with for instance fluorescence detectors [15], allows to measure simultaneously the primary energy and  $X_{max}$  and can therefore be used to determine the absolute value of the average nuclear mass as a function of energy (cf. Sec. IV). The *elongation rate* [16]–[18],  $d\langle X_{max} \rangle/d(\lg E) \propto -d(\lg A)/d(\lg E)$ , can be used to study the change of the primary cosmic ray composition with energy.

The number of muons,  $N_\mu$ , from the decay of charged pions that can be detected by particle detectors on ground is given by

$$N_\mu = (E_0/\epsilon_{ch})^\beta A^{1-\beta} \quad (2)$$

where again the properties of hadronic interactions are hidden in a single number,  $\beta$ , that is proportional to the logarithm of the charged meson multiplicity. Given a similar relation for the number of electrons on ground, a detector that is capable to distinguish muons and electrons can therefore disentangle the energy and mass of cosmic primaries on a statistical basis.

The simple Heitler approach is very useful to understand the principles of air shower physics, but of course in practice experiments employ full Monte Carlo simulations of air showers with for instance CORSIKA [19] to interpret their data. These simulations are however of limited predictive power, as they need to rely on models of hadronic interactions at energies beyond man-made accelerators. The related uncertainties are the source of considerable systematic uncertainties for the interpretation of air shower data (see [20], [21]).

Since the energy estimated from the integral of the electromagnetic longitudinal air shower development depends only very little on details of hadronic interactions [22], [23], modern air shower arrays like the Pierre Auger Observatory [24] or Telescope Array [25] use a *hybrid* approach to calibrate the

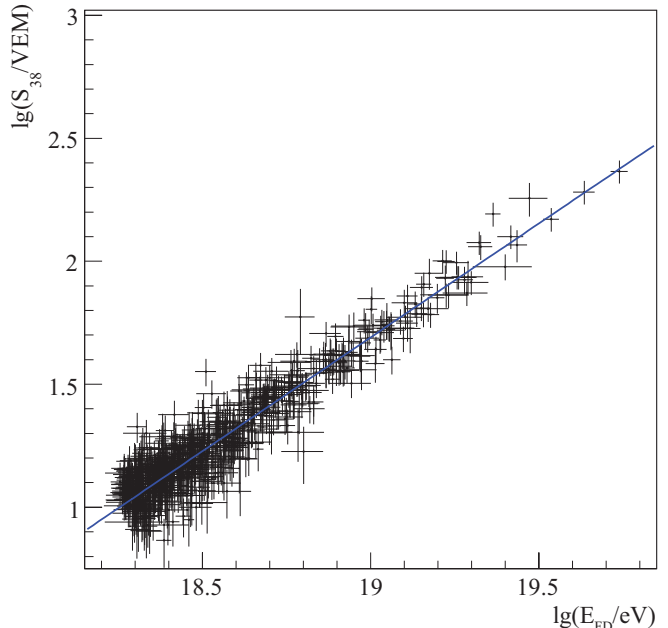


Fig. 2. Energy calibration of the surface detector of the Pierre Auger Observatory [26]: Shower size,  $S_{38}$ , as a function of energy,  $E_{FD}$ , measured with the fluorescence detector.

energy scale of their surface detector with the energy estimate of a fluorescence detector. An example is shown in Fig. 2, where the expected power-law dependence of the number of ground particles on the primary energy (Eq. (2)) can be seen.

### III. FROM GALACTIC TO EXTRA-GALACTIC COSMIC RAYS

The standard explanation for the knee-feature in the cosmic ray all-particle flux between  $10^{15}$  and  $10^{16}$  eV is that it marks the beginning of the end of the galactic cosmic ray spectrum due to the escape of the high energy charged particles from the magnetic confinement within the galaxy and/or the reach of the maximum energy of galactic accelerators (presumably supernova remnants). Although the current experimental data can not rule out alternative explanations for the knee (eg. [27]–[31]), extrapolations of the low energy cosmic ray data with a rigidity dependent cut off  $\propto Z \cdot E_c$  can describe the existing data very well [32], [33]. Moreover, the deconvoluted galactic mass spectra measured with KASCADE [34] show distinct knees for each elemental component, compatible with a rigidity dependent knee.

Since  $E_c$  is of the order of PeV, it follows that above energies of several  $10^{18}$  eV, the detected cosmic particles must be of extra-galactic origin. As a corollary, this assumption explains the lack of an observation of a strong anisotropy that would be expected for charged particles with a large gyro-radius at this energy.

In the following we will describe three different models of the transition from galactic to extra-galactic cosmic rays (see [35]–[38] for recent reviews on this topic). Common to all of these models is that the properties of extra-galactic

cosmic ray sources are described by just four parameters: the source emissivity (needed to adjust the overall normalization), the spectral index  $\gamma_0$  of the energy spectrum at the source, the maximum energy  $Z \cdot E_c$  the source is able to accelerate particles to and the cosmological source evolution parameter  $m$ , that describes the source density  $n$  as a function of redshift  $z$ ,  $dn/dz \propto (1+z)^m$ . In order to simplify the discussion, we will restrict ourselves to the uniform source distribution model ( $m = 0$ ) and assume that  $E_c$  is large enough to have no observational consequence within the statistical precision of current experiments. Furthermore we will assume the simple phenomenological rigidity-dependent parameterization from [32] to describe the 'standard' galactic cosmic ray component. Since there is an obvious disagreement of the measured ultra-high energy spectra [39]–[41] (cf. Fig 1), their energy scale will be 'adjusted' accordingly within the quoted systematic uncertainties.

### A. Dip Model

In the so-called *dip model* [42], all extragalactic cosmic rays are assumed to be protons (at least after they escaped from their sources [43]) and the ankle feature is caused by energy losses suffered during the propagation to earth.

First of all, the expansion of the universe causes adiabatic losses that are important for very distant sources (cf. Fig. 3a). Since it affects all energies equally, it does not change the spectral index observed at earth.

A more important effect is the interaction of the cosmic ray protons with the photons of the cosmic microwave background radiation. At lower energies, the production of  $e^+e^-$ -pairs through the Bethe-Heitler process is the dominant source of energy loss (cf. Fig. 3b) and at energies above  $10^{19.5}$  eV, the photon-proton center of mass energy is large enough for resonant photo-pion production, that gives rise to large energy losses [3] even for very close source (cf. Fig. 3c).

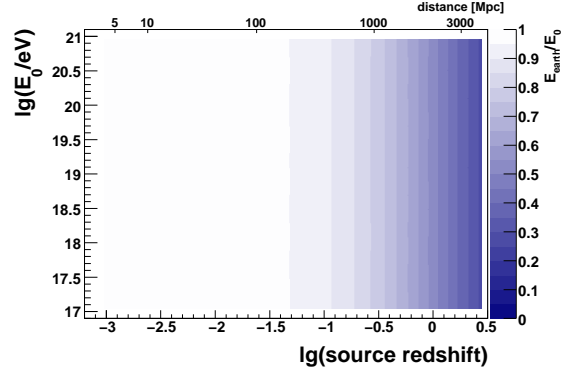
As can be seen in Fig. 4a, the dip model can describe the data rather well. The transition between the galactic and extragalactic cosmic ray component is at low energies just above 0.1 EeV and produces the somewhat less prominent feature called the *second knee* [44].

Thus the dip model is a very economic approach in terms of assumptions, as it can explain all features in the cosmic ray energy spectrum in terms of the well understood interactions of protons with photons and predicts a transition energy that is low enough to be compatible with current estimates of the maximum energy of galactic accelerators [45].

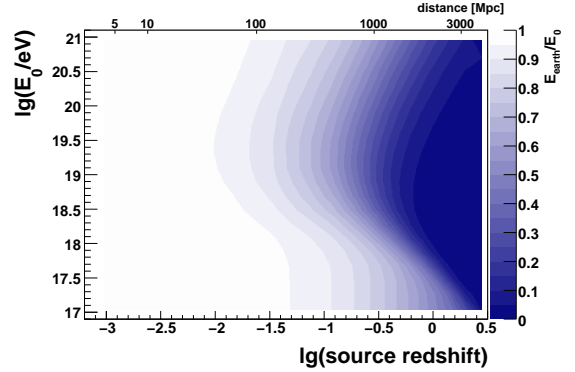
However, the hard injection spectrum at the source is problematic in terms of the overall energy luminosity of extragalactic sources if extrapolated to low energies. Therefore an 'artificial' softening of the spectrum below a certain energy is usually introduced [46] (not shown in Fig. 4a).

### B. Mixed Composition Model

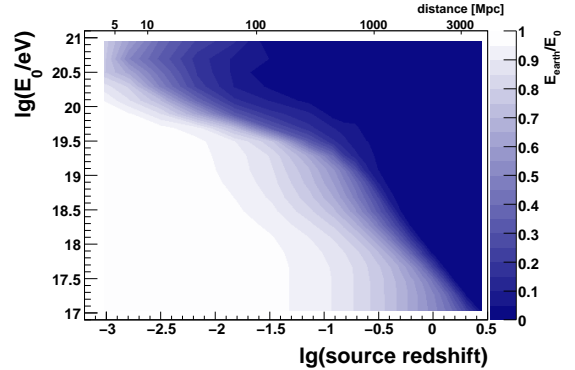
The dip-model works only for a pure proton beam since an admixture of heavier nuclei with a fraction of  $\geq 15\%$  diminishes the agreement with the data considerably. This is,



(a) redshift



(b) redshift and pair-production



(c) redshift, pair- and photo-pion-production

Fig. 3. Fractional energy at earth, ( $E_{\text{earth}}/E_0$ ), of protons with initial energy  $E_0$  as a function of the source distance/redshift (CRPROPA [47] calculation).

because the threshold for  $e^+e^-$ -production is proportional to the energy per nucleon and thus only relevant for protons at the energies of the ankle. Instead, cosmic ray nuclei lose their energy predominantly due to photo-disintegration at the giant dipole resonance [48]. The mean free path for photo-disintegration scales with the Lorentz-factor of the particle and drops rapidly above  $\Gamma \gtrsim 10^9$ .

In *mixed composition models* [49], [50] the extra-galactic cosmic ray composition is assumed to be equal to the one

measured at low energies in our galaxy. Due to the Lorentz-factor dependence of the energy loss, the individual spectra of nuclei with mass  $A$  are subsequently suppressed at energies above  $\gtrsim A \cdot 10^{18}$  eV.

As in case of the dip-model, this ansatz gives a good description of the existing data (cf. Fig. 4b), but with a much softer extra-galactic source spectrum. The transition from galactic to extra-galactic cosmic rays is at about a factor 10 higher energies close to 1 EeV and correspondingly, this model needs galactic sources with a higher maximum acceleration energy than the dip-model.

### C. Ankle Model

Finally, the traditional way to reproduce the ankle-feature is to model it as the intersection of a flat extra-galactic component with a steep galactic component (see for instance [52], [53]). In that case, as can be seen in Fig. 4c), the galactic cosmic ray spectrum extends to energies well above several EeV and thus would require a significant modification of the simple rigidity model of the knee.

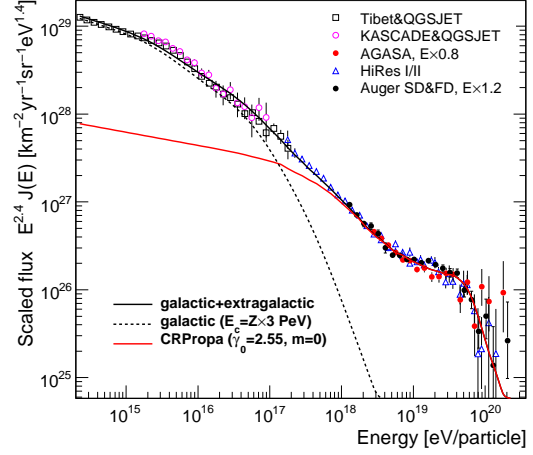
## IV. COMPOSITION OF UHECRS

All of the transition models explained in the last section give a similar good description of the measured cosmic ray spectra under very different astrophysical assumptions. Since they differ substantially in the predicted cosmic ray composition as a function of energy, this observable is the key to distinguish between the models.

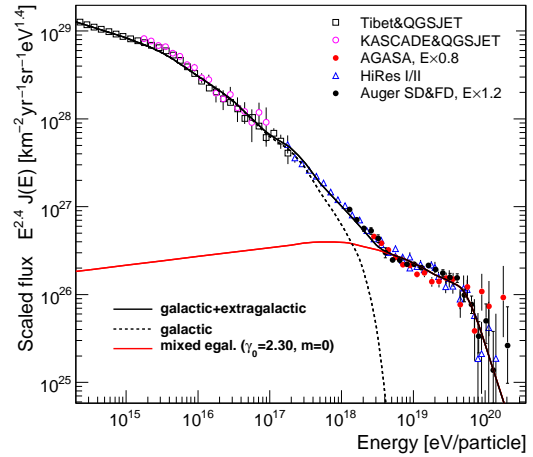
The mass composition estimated from surface detector observables is compatible with large contributions from heavy elements up to the highest energies (see [54], [55]). These estimates rely to a large extent on an accurate prediction of the number of muons (cf. Eq. 2) in air showers. However, modern hadronic interaction models differ by as much as 30% in the number of muons on ground [56], [57]. Moreover, the application of air shower universality to data from the Pierre Auger Observatory suggests, that current air shower simulations systematically underestimate the number of muons [58], [59].

The maximum of the longitudinal development of the electromagnetic component of air showers (cf. Eq. 1) provides a composition sensitivity that is somewhat less dependent on the details of hadronic interactions. As can be seen in Fig. 5a, all current air shower models give similar predictions of  $\langle X_{\max} \rangle$  between 0.1 and 10 EeV. It is however worthwhile noting that this might be a mere coincidence, since also the predictions of the depth of the shower maximum can be changed significantly, if some more drastic (though experimentally not excluded) modifications of the hadronic interactions at high energies are assumed [60]–[63].

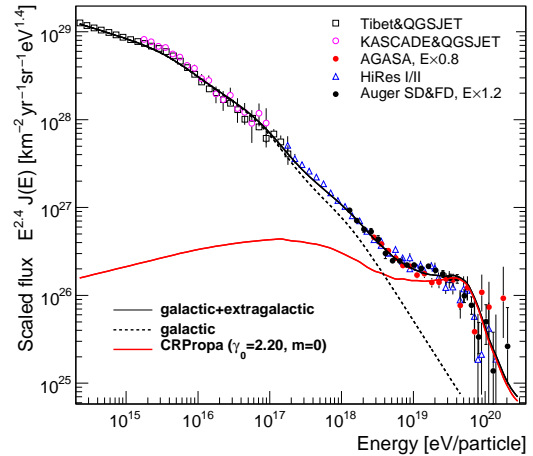
The shower maximum can be directly measured by fluorescence detectors, that can infer the longitudinal shower development from the observation of fluorescence and Cherenkov light emitted by the shower as a function of height [75]. Observations of the lateral distribution of Cherenkov light at ground and its pulse shape are sensitive to  $X_{\max}$  as well [76].



(a) Extragalactic protons

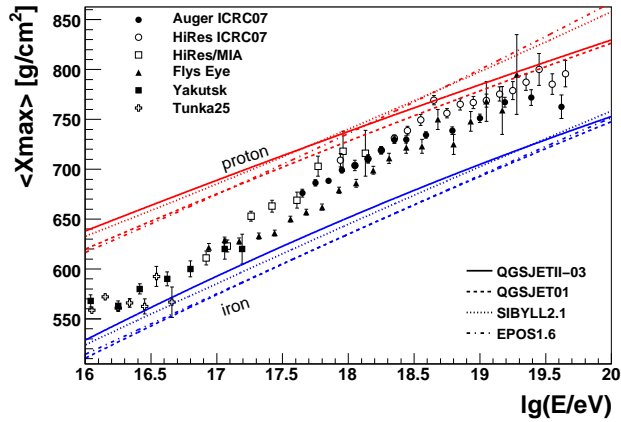


(b) Mixed Composition (adopted from [49])

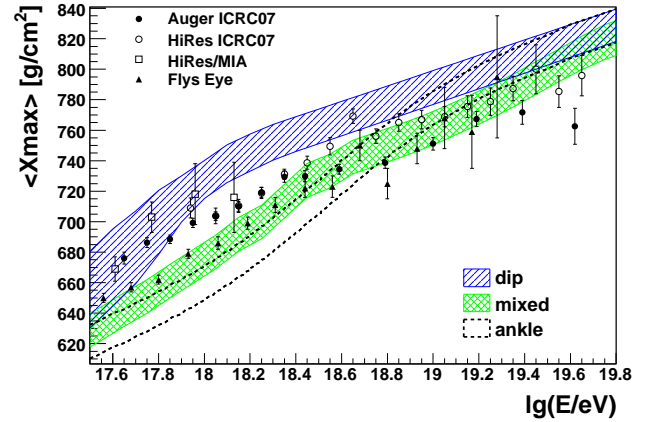


(c) Transition at the ankle

Fig. 4. Models of the transition from galactic to extra-galactic cosmic rays vs. measurements of the all particle flux [34], [39]–[41], [51].



(a) Comparison to simulations [64] for proton and iron induced air showers using different hadronic interaction models [57], [65]–[67]



(b) Comparison to transition models (calculations taken from [68], bands indicate the uncertainty from interaction models).

Fig. 5. Measurements of  $\langle X_{\max} \rangle$  from Cherenkov [69], [70] and fluorescence [71]–[74] detectors

Measurements of the average of  $X_{\max}$  over almost three orders of magnitude in energy are shown in Fig. 5a together with predictions from air shower simulations for proton and iron primaries. As can be seen, the data are indeed showing a trend from a heavy composition at low energies towards a light one at high energies, as would be expected from the transition models introduced in the last section. There are however systematic differences between the different experiments. The HiRes data, for instance, is compatible with a pure proton composition if compared to the QGSJET prediction, whereas the data from the Pierre Auger Observatory favors a mixed composition at all energies.

A direct comparison of the data to the  $\langle X_{\max} \rangle$  predicted by the dip-, ankle- and mixed-composition model is shown in Fig. 5b. Obviously, none of the three models gives a satisfactory description of the data, neither in shape nor the absolute  $\langle X_{\max} \rangle$  value, but note that mixed-composition models have in principle enough parameters to be adjusted to the data.

Until now we only discussed the average value of the shower maximum. The *distribution* of  $X_{\max}$  can potentially constrain the mass composition of cosmic rays even better. In the naive superposition model, one would expect that nuclei with mass  $A$  have smaller shower-to-shower fluctuations by a factor of  $1/\sqrt{A}$ . Correctly accounting for nuclear fragmentation leads to somewhat larger fluctuations of nucleus-induced showers [77]–[79], but still the width of the  $X_{\max}$  distribution of iron showers is about a factor three smaller than that for proton (about 20 and 60 g/cm<sup>2</sup> at 1 EeV respectively). The analysis of the  $X_{\max}$  distribution requires however a good understanding of the detector resolution and corresponding composition estimates from the  $X_{\max}$  fluctuations are still contradictory (for instance pure proton in [80] and mixed in [81] above 1 EeV).

## V. THE END OF THE COSMIC RAY SPECTRUM

More than forty years after Greisen, Zatsepin and Kuzmin [3] (GZK) predicted a suppression of the cosmic ray flux due to interactions with the cosmic microwave background (CMB) radiation and its existence has now finally been established with high significance by HiRes and the Pierre Auger Observatory [26], [40] (cf. Fig. 6). Furthermore, Auger reported an anisotropy of the arrival direction of cosmic rays above 60 EeV [82] and set a limit of  $\leq 2\%$  on the fraction of photons above 10 EeV. The latter excludes most of the *top-down* scenarios, i.e. cosmic ray production in decays of ultra-massive particles (see eg. [83]), that were motivated by the absence of a GZK feature in the AGASA spectrum [39]. The onset of the anisotropy at about the same energy as the GZK threshold suggests that the suppression is indeed due to propagation effects and not because the maximum energy of the sources is reached: If sources are isotropically distributed on large scales, local anisotropies can not be detected in a transparent universe, but only if propagation losses limit the distance from which cosmic rays can reach earth (the so-called *GZK-horizon*).

It is a curiosity, that the thresholds for photo-pion production of protons with photons of the CMB is at a similar energy as the giant dipole resonance for iron nuclei. As can be seen in Fig. 6, the current statistical precision of the flux measurements at ultra-high energies is not sufficient to distinguish between the predictions for the spectral shape for cosmic rays with a pure proton [80] and iron [84] composition at the source. (It is worthwhile noting that the measured spectra are not corrected for the corresponding experimental energy resolution and if a deconvolution was applied 'true' shape of the flux suppression would get steeper). A possible way to resolve this degeneracy in the near future would be the detection of photons [85] or neutrinos [86] originating from the decay of pions produced during the proton propagation (nuclei are expected to produce much less neutrinos [87]–[89]).

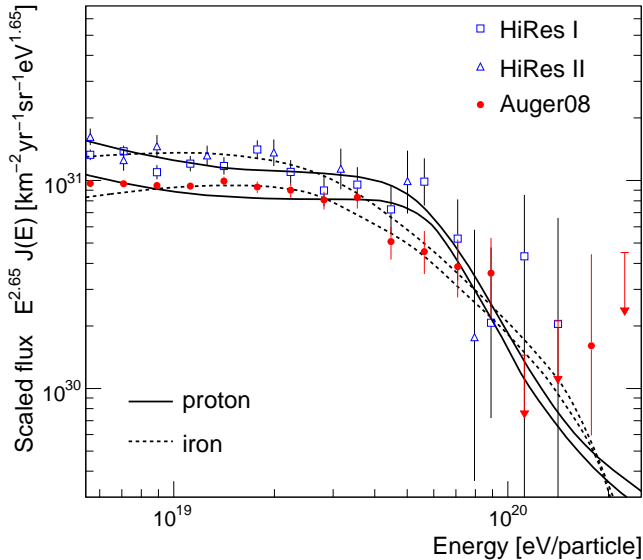


Fig. 6. Measured flux at ultra-high energies compared to predictions for propagated proton and iron primaries (lines adapted from [80] and [84]).

The anisotropy reported by the Pierre Auger Observatory was established by correlation of the arrival direction of cosmic rays and the location of active galactic nuclei (AGNs) [90] (cf. Fig.7) within  $3.1^\circ$ . This angular scale is compatible with the deflections expected for protons in the galactic magnetic field (see for instance [91]), but from the current statistics it is not possible to distinguish if the AGNs from [90] are indeed the source of ultra-high energy cosmic rays or just a tracer of the true source distribution like the super-galactic plane [92], the large scale structure of nearby matter [93] or even a few sources producing nuclei of intermediate mass [94] that are spread out by magnetic fields. Note that a follow-up analysis of HiRes did not show a correlation [95], which may, however, be explained by the different energy scales of the two experiments.

## VI. OUTLOOK

The last years have brought a wealth of new precise data on cosmic rays above the knee, especially at ultra-high energies collected by the southern part of the Pierre Auger Observatory. Since its construction was just finished this year, one can soon expect updated results with increased statistics. Its northern part is planned to be built in Colorado, USA, and will increase the exposure of the observatory by a factor of seven and provide full sky coverage for particle astronomy [96]. The space-borne experiments TUS [97] and JEM-EUSO [98] will observe air showers from space and investigate the region above the GZK cutoff.

At intermediate energies, the hybrid Telescope Array [25] started data taking and will study the region around the ankle with fluorescence detectors and a scintillator array. Both, the

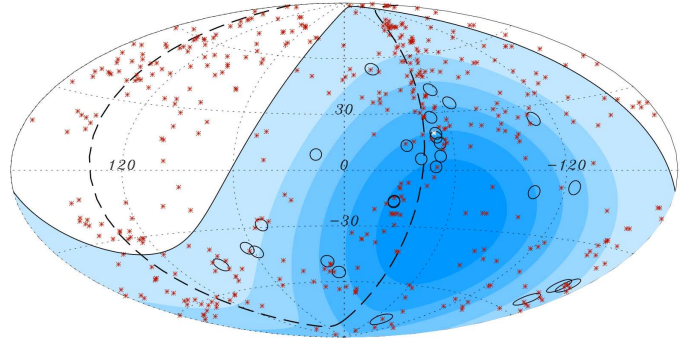


Fig. 7. Arrival directions of cosmic rays ( $E > 60$  EeV) measured by the Pierre Auger Observatory (open circles) within its acceptance (shaded area) and location of active galactic nuclei (small dots) [82].

Pierre Auger Observatory and Telescope Array aim at covering the transition region of galactic to extragalactic cosmic rays down to  $10^{17}$  eV by using fluorescence telescopes with enlarged field of views and shielded particle counters [99]–[101]. The construction of the low energy enhancement of the southern Auger site is almost finished and ‘first light’ is expected in early 2009. Finally, the end of the galactic cosmic ray spectrum is currently observed by IceTop [102] and KASCADE-Grande [103] down to energies of  $10^{16}$  eV.

This new cosmic ray detectors will thus cover more than four orders of magnitude from the knee up to beyond the GZK cutoff. A number of laboratory experiments will provide additional measurements to lower the systematic uncertainties of the cosmic ray measurements: Many of the modern detectors use fluorescence detectors to calibrate their energy scale and the absolute value of the fluorescence yield in air is one of the major contributions to the current energy scale uncertainties of HiRes and Auger. It is currently re-measured under various atmospheric conditions by several groups [104]. Furthermore, in order to diminish the uncertainties of the hadronic interaction models employed to interpret the cosmic ray data, more data from controlled interactions at accelerators are collected. The NA61 experiment [105] at the Super Proton Synchrotron at CERN will measure pion-carbon interactions above 300 GeV that are important for the last stages of the air shower development [106] and LHCf [107], TOTEM [108] and CASTOR [109] at the Large Hadron Collider will provide data on particle production in the forward region and the proton-proton cross section at center of mass energies corresponding to  $10^{17}$  eV in terms of primary cosmic ray energies.

## REFERENCES

- [1] G. V. Kulikov and G. B. Khristiansen, *Zh. Eksp. Teor. Fiz.*, vol. 35, p. 635, 1958.
- [2] J. Linsley, "Primary cosmic rays of energy  $10^{17}$  to  $10^{20}$  eV, the energy spectrum and arrival directions," *Proc. 8th ICRC, Jaipur*, vol. 4, p. 77, 1963.
- [3] K. Greisen, *Phys. Rev. Lett.*, vol. 16, pp. 748–750, 1966.  
G. T. Zatsepin and V. A. Kuzmin, *JETP Lett.*, vol. 4, pp. 78–80, 1966.
- [4] [press.web.cern.ch/press/PressReleases/Releases2008/PR08.08E.html](http://press.web.cern.ch/press/PressReleases/Releases2008/PR08.08E.html).
- [5] J. Linsley, *Phys. Rev. Lett.*, vol. 10, pp. 146–148, 1963.
- [6] D. Bird et al. [Fly's Eye Collaboration], *Astrophys. J.*, vol. 441, pp. 144–150, 1995.
- [7] J. Matthews et al. [Pierre Auger Collaboration], "A description of some ultra high energy cosmic rays observed with the Pierre Auger Observatory," *Proc. 29th ICRC, Pune* (2005).
- [8] A. A. Watson, "Highlights from the Pierre Auger Observatory - the birth of the hybrid era," *Proc. 30th ICRC, Merida* (2007), arXiv:0801.2321 [astro-ph].
- [9] R. Engel, *Nucl. Phys. Proc. Suppl.*, vol. 122, pp. 437–446, 2003.
- [10] C. Amsler et al. [Particle Data Group], *Phys. Lett.*, vol. B667, p. 1, 2008.
- [11] J. Carlson and J. Oppenheimer, *Physical Review*, vol. 51, pp. 220–231, 1937.
- [12] W. Heitler, *The Quantum Theory of Radiation*. Oxford University Press, 1954.
- [13] J. Matthews, *Astroparticle Physics*, vol. 22, pp. 387–397, 2005.
- [14] J. R. Hoerandel, *Mod. Phys. Lett.*, vol. A22, pp. 1533–1552, 2007.
- [15] L. G. Porter, J. C. Earnshaw, E. Tielsch-Cassel, J. C. Ahlstrom, and K. Greisen, *Nucl. Instrum. Meth.*, vol. 87, pp. 87–92, 1970.
- [16] J. Linsley, "Structure of Large Air Showers at Depth  $834 \text{ g/cm}^2$ : Applications," *Proc. 12th ICRC, Budapest*, vol. 12, p. 89, 1977.
- [17] T. K. Gaisser, T. J. L. McComb, and K. E. Turver, "Elongation Rate of Air Showers and Implications for  $10^{17}$ – $10^{18}$  eV Particle Interactions," *Proc. 16th ICRC, Tokyo*, vol. 9, p. 275, 1979.
- [18] J. Linsley and A. A. Watson, *Phys. Rev. Lett.*, vol. 46, pp. 459–463, 1981.
- [19] D. Heck, G. Schatz, T. Thouw, J. Knapp, and J. N. Capdevielle, "CORSIKA: A Monte Carlo code to simulate extensive air showers," *forschungszentrum Karlsruhe Report, FZKA-6019* (1998).
- [20] J. Knapp, D. Heck, S. J. Sciutto, M. T. Dova, and M. Risse, *Astropart. Phys.*, vol. 19, pp. 77–99, 2003.
- [21] T. Pierog, R. Engel, and D. Heck, *Czech. J. Phys.*, vol. 56, pp. A161–A172, 2006.
- [22] H. M. J. Barbosa, F. Catalani, J. A. Chinellato, and C. Dobrigkeit, *Astropart. Phys.*, vol. 22, pp. 159–166, 2004.
- [23] T. Pierog, R. Engel, D. Heck, S. Ostapchenko, and K. Werner, "Latest Results from the Air Shower Simulation Programs CORSIKA and CONEX," *Proc. 30th ICRC, Merida* (2007), arXiv:0802.1262 [astro-ph].
- [24] J. Abraham et al. [Pierre Auger Collaboration], *Nucl. Instrum. Meth.*, vol. A523, pp. 50–95, 2004.
- [25] H. Kawai [TA Collaboration], *Nucl. Phys. Proc. Suppl.*, vol. 175–176, pp. 221–226, 2008.
- [26] J. Abraham et al. [Pierre Auger Collaboration], *Phys. Rev. Lett.*, vol. 101, p. 061101, 2008.
- [27] S. I. Nikolsky, *Nucl. Phys. Proc. Suppl.*, vol. 39A, pp. 228–234, 1995.
- [28] A. D. Erlykin and A. W. Wolfendale, *J. Phys.*, vol. G23, pp. 979–989, 1997.
- [29] M. T. Dova, L. N. Epele, and J. D. Swain, "Massive relic neutrinos in the galactic halo and the knee in the cosmic ray spectrum," arXiv:0112191 [astro-ph].
- [30] J. Candia, L. N. Epele, and E. Roulet, *Astropart. Phys.*, vol. 17, pp. 23–33, 2002.
- [31] A. Dar and A. De Rujula, *Phys. Rept.*, vol. 466, pp. 179–241, 2008.
- [32] J. R. Hoerandel, *Astropart. Phys.*, vol. 19, pp. 193–220, 2003.
- [33] E. G. Berezhko and H. J. Voelk, "Spectrum of cosmic rays, produced in supernova remnants," 2007, arXiv:0704.1715 [astro-ph].
- [34] T. Antoni et al. [KASCADE Collaboration], *Astropart. Phys.*, vol. 24, pp. 1–25, 2005.
- [35] A. M. Hillas, "Cosmic rays: Recent progress and some current questions," arXiv:0607109 [astro-ph].
- [36] T. Stanev, *Nucl. Phys. Proc. Suppl.*, vol. 168, pp. 252–257, 2007.
- [37] V. Berezhinsky, "Transition from galactic to extragalactic cosmic rays," *Proc. 30th ICRC, Merida* (2007), arXiv:0710.2750 [astro-ph].
- [38] C. De Donato and G. A. Medina-Tanco, "Experimental constraints on the astrophysical interpretation of the cosmic ray Galactic-extragalactic transition region," arXiv:0807.4510 [astro-ph].
- [39] M. Takeda et al. [AGASA Collaboration], *Astropart. Phys.*, vol. 19, pp. 447–462, 2003.
- [40] R. Abbasi et al. [HiRes Collaboration], *Phys. Rev. Lett.*, vol. 100, p. 101101, 2008.
- [41] T. Yamamoto et al. [Pierre Auger Collaboration], "The UHECR spectrum measured at the Pierre Auger Observatory and its astrophysical implications," *Proc. 30th ICRC, Merida* (2007), arXiv:0707.2638 [astro-ph].
- [42] V. S. Berezhinsky and S. I. Grigoreva, *Bull. Russ. Acad. Sci. Phys.*, vol. 51N10, pp. 111–113, 1987.  
V. Berezhinsky, A. Z. Gazizov, and S. I. Grigorieva, *Phys. Rev.*, vol. D74, p. 043005, 2006.
- [43] G. Sigl and E. Armengaud, *JCAP*, vol. 0510, p. 016, 2005.
- [44] D. R. Bergman and J. W. Belz, *J. Phys.*, vol. G34, p. R359, 2007.
- [45] E. G. Berezhko and L. T. Ksenofontov, *J. Exp. Theor. Phys.*, vol. 89, pp. 391–403, 1999.
- [46] V. S. Berezhinsky, S. I. Grigorieva, and B. I. Hnatyk, *Astropart. Phys.*, vol. 21, pp. 617–625, 2004.
- [47] E. Armengaud, G. Sigl, T. Beau, and F. Miniati, *Astropart. Phys.*, vol. 28, pp. 463–471, 2007.
- [48] E. Khan et al., *Astropart. Phys.*, vol. 23, pp. 191–201, 2005.
- [49] D. Allard, E. Parizot, and A. V. Olinto, *Astropart. Phys.*, vol. 27, pp. 61–75, 2007.
- [50] D. Hooper, S. Sarkar, and A. M. Taylor, *Astropart. Phys.*, vol. 27, pp. 199–212, 2007.
- [51] M. Amenomori, et al. [Tibet AS $\gamma$  Collaboration], *Astrophysical Journal*, vol. 678, pp. 1165–1179, 2008.
- [52] T. Wibig and A. W. Wolfendale, *J. Phys.*, vol. G31, pp. 255–264, 2005.
- [53] J. N. Bahcall and E. Waxman, *Phys. Lett.*, vol. B556, pp. 1–6, 2003.
- [54] M. T. Dova, M. E. Mancenido, A. G. Mariazzi, T. P. McCauley, and A. A. Watson, *Astropart. Phys.*, vol. 21, pp. 597–607, 2004.
- [55] A. A. Watson, *Nucl. Phys. Proc. Suppl.*, vol. 136, pp. 290–300, 2004.
- [56] H.-J. Drescher, M. Bleicher, S. Soff, and H. Stoecker, *Astropart. Phys.*, vol. 21, pp. 87–94, 2004.
- [57] T. Pierog and K. Werner, *Phys. Rev. Lett.*, vol. 101, p. 171101, 2008.
- [58] F. Schmidt, M. Ave, L. Cazon, and A. S. Chou, *Astropart. Phys.*, vol. 29, pp. 355–365, 2008.
- [59] R. Engel et al. [Pierre Auger Collaboration], "Test of hadronic interaction models with data from the Pierre Auger Observatory," *Proc. 30th ICRC, Merida* (2007), arXiv:0706.1921 [astro-ph].
- [60] H.-J. Drescher, *Nucl. Phys. Proc. Suppl.*, vol. 151, pp. 163–166, 2006.
- [61] R. Ulrich et al., "On the measurement of the proton-air cross section using cosmic ray data," arXiv:0709.1392 [astro-ph].
- [62] J. Alvarez-Muniz, J. D. de Deus, and C. Pajares, "Strong colour fields and cosmic ray showers at ultra-high energies," arXiv:0804.4751 [hep-ph].
- [63] T. Wibig, "Ultra High-Energy Interaction of CR protons," these proceedings, arXiv:0810.5281 [hep-ph].
- [64] T. Bergmann et al., *Astropart. Phys.*, vol. 26, pp. 420–432, 2007.
- [65] N. N. Kalmykov, S. S. Ostapchenko, and A. I. Pavlov, *Nucl. Phys. Proc. Suppl.*, vol. 52B, pp. 17–28, 1997.
- [66] R. Engel, T. K. Gaisser, T. Stanev, and P. Lipari, "Air shower calculations with the new version of SIBYLL," *Proc. 26th ICRC, Salt Lake City*, p. 415, 1999.
- [67] S. Ostapchenko, *Nucl. Phys. Proc. Suppl.*, vol. 151, p. 143, 2006.
- [68] D. Allard, A. V. Olinto, and E. Parizot, "Signatures of the extragalactic cosmic-ray source composition from spectrum and shower depth measurements," arXiv:0703633 [astro-ph].
- [69] S. Knurenko et al. [Yakutsk Collaboration], "Lateral Distribution of Cherenkov Radiation in the Energy Region of  $10^{15}$  -  $10^{17}$  eV," *Proc. 27th ICRC, Hamburg*, vol. 1, p. 177, 2001.
- [70] V. V. Prosin [Tunka-25 Collaboration], "Cosmic Ray Mass Composition by the Data of Tunka-25 EAS Cherenkov Array," these proceedings.
- [71] D. Bird et al. [HiRes Collaboration], *Phys. Rev. Lett.*, vol. 71, pp. 3401–3404, 1993.
- [72] T. Abu-Zayyad et al. [HiRes/MIA Collaboration], *Astrophys. J.*, vol. 557, pp. 686–699, 2001.

- [73] Y. Fedorova et al. [HiRes Collaboration], “Cosmic Rays Composition Measurements by the HiRes Stereo,” Proc. 30th ICRC, Merida (2007).
- [74] M. Unger et al. [Pierre Auger Collaboration], “Study of the Cosmic Ray Composition above 0.4 EeV using the Longitudinal Profiles of Showers observed at the Pierre Auger Observatory,” Proc. 30th ICRC, Merida (2007), arXiv:0706.1495 [astro-ph].
- [75] M. Unger, B. R. Dawson, R. Engel, F. Schsler, and R. Ulrich, *Nucl. Instrum. Meth.*, vol. A588, pp. 433–441, 2008.
- [76] J. R. Patterson and A. M. Hillas, *J. Phys.*, vol. G9, pp. 323–337, 1983. J. R. Patterson and A. M. Hillas, *J. Phys.*, vol. G9, pp. 1433–1452, 1983.
- [77] J. Engel, T. K. Gaisser, T. Stanev, and P. Lipari, *Phys. Rev.*, vol. D46, pp. 5013–5025, 1992.
- [78] N. N. Kalmykov and S. S. Ostapchenko, *Phys. Atom. Nucl.*, vol. 56, pp. 346–353, 1993.
- [79] B. Schatz et al., *J. Phys.*, vol. G20, pp. 1267–1281, 1994.
- [80] R. Aloisio, V. Berezhinsky, P. Blasi, and S. Ostapchenko, *Phys. Rev.*, vol. D77, p. 025007, 2008.
- [81] S. P. Knurenko et al. [Yakutsk Collaboration], *Int. J. Mod. Phys.*, vol. A20, pp. 6894–6896, 2005.
- [82] J. Abraham et al. [Pierre Auger Collaboration], *Science*, vol. 318, pp. 938–943, 2007. J. Abraham et al. [Pierre Auger Collaboration], *Astropart. Phys.*, vol. 29, pp. 188–204, 2008. E. M. Santos, “Anisotropy Studies with Auger,” these proceedings.
- [83] M. Kachelriess, “The rise and fall of top-down models as main UHECR sources,” arXiv:0810.3017 [astro-ph].
- [84] D. Allard et al., *JCAP*, vol. 0810, p. 033, 2008.
- [85] M. Risse and P. Homola, *Mod. Phys. Lett.*, vol. A22, pp. 749–766, 2007.
- [86] R. Engel, D. Seckel, and T. Stanev, *Phys. Rev.*, vol. D64, p. 093010, 2001.
- [87] M. Ave, N. Busca, A. V. Olinto, A. A. Watson, and T. Yamamoto, *Astropart. Phys.*, vol. 23, pp. 19–29, 2005.
- [88] D. Hooper, A. Taylor, and S. Sarkar, *Astropart. Phys.*, vol. 23, pp. 11–17, 2005.
- [89] L. A. Anchordoqui, H. Goldberg, D. Hooper, S. Sarkar, and A. M. Taylor, *Phys. Rev.*, vol. D76, p. 123008, 2007.
- [90] M. Veron-Cetty and P. Veron, *Astron. Astrophys.*, vol. 22, pp. 773–777, 2006.
- [91] J. Alvarez-Muniz, R. Engel, and T. Stanev, *Astrophys. J.*, vol. 572, pp. 185–201, 2001.
- [92] T. Stanev, “A comment on the Auger events correlation with AGN,” arXiv:0805.1746 [astro-ph].
- [93] T. Kashti and E. Waxman, *JCAP*, vol. 0805, p. 006, 2008.
- [94] T. Wibig and A. W. Wolfendale, “Heavy Cosmic Ray Nuclei from Extragalactic Sources above ‘The Ankle’,” arXiv:0712.3403 [astro-ph].
- [95] R. Abbasi et al. [HiRes Collaboration], “Search for Correlations between HiRes Stereo Events and Active Galactic Nuclei,” arXiv:0804.0382 [astro-ph].
- [96] D. Nitz [Pierre Auger Collaboration], “The Northern Site of the Pierre Auger Observatory,” Proc. 30th ICRC, Merida (2007), arXiv:0706.3940 [astro-ph].
- [97] V. I. Abrashkin et al. [TUS Collaboration], *Int. J. Mod. Phys.*, vol. A20, pp. 6865–6868, 2005.
- [98] P. Gorodetzky [JEM-EUSO Collaboration], “JEM-EUSO,” these proceedings.
- [99] H. O. Klages [Pierre Auger Collaboration], “HEAT: Enhancement telescopes for the Pierre Auger Southern Observatory,” Proc. 30th ICRC, Merida (2007).
- [100] A. Etchegoyen [Pierre Auger Collaboration], “AMIGA, Auger Muons and Infill for the Ground Array,” Proc. 30th ICRC, Merida (2007), arXiv:0710.1646 [astro-ph].
- [101] G. Thomson et al. [TA Collaboration], “Physics of the TALE Experiment,” Proc. 30th ICRC, Merida (2007).
- [102] S. Klepser [IceTop Collaboration], “First Results from the IceTop Air Shower Array,” these proceedings, arXiv:0811.1671 [astro-ph].
- [103] A. Chiavassa [KASCADE-Grande Collaboration], “The KASCADE-Grande experiment: an overview,” these proceedings.
- [104] F. Arqueros, J. R. Hoerandel, and B. Keilhauer, “Air Fluorescence Relevant for Cosmic-Ray Detection - Summary of the 5th Fluorescence Workshop, El Escorial 2007,” arXiv:0807.3760 [astro-ph].
- [105] N. Abragall et al. [NA61 Collaboration], “Report from the NA61/SHINE experiment at the CERN SPS,” CERN-OPEN-2008-012.
- [106] C. Meurer, J. Bluemer, R. Engel, A. Haungs, and M. Roth, *Czech. J. Phys.*, vol. 56, p. A211, 2006.
- [107] Y. Muraki [LHCf Collaboration], “Current status of the LHCf experiment,” these proceedings.
- [108] G. Anelli [TOTEM Collaboration], *JINST*, vol. 3, p. S08007, 2008.
- [109] X. Aslanoglou et al. [CMS Collaboration], *Eur. Phys. J.*, vol. C52, pp. 495–506, 2007.